# Accepted Manuscript

Should environmental effects be included when performing QTAIM calculations on actinide systems? A comparison of QTAIM metrics for $Cs_2UO_2Cl_4$, $U(Se_2PPh_2)_4$ and $Np(Se_2PPh_2)_4$ in gas phase, COSMO and PEECM

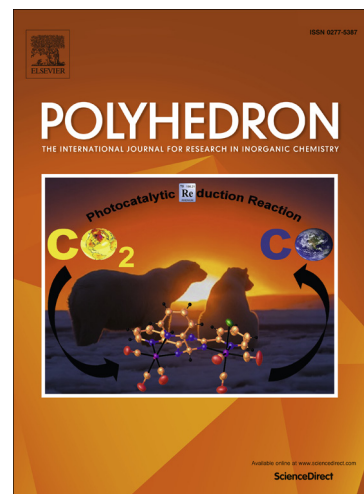Joseph P.W. Wellington, Andrew Kerridge, Nikolas Kaltsoyannis

Please cite this article as: J.P.W. Wellington, A. Kerridge, N. Kaltsoyannis, Should environmental effects be included when performing QTAIM calculations on actinide systems? A comparison of QTAIM metrics for $Cs_2UO_2Cl_4$, $U(Se_2PPh_2)_4$ and $Np(Se_2PPh_2)_4$ in gas phase, COSMO and PEECM, *Polyhedron* (2016), doi: http://dx.doi.org/10.1016/j.poly.2016.02.048

# Should environmental effects be included when performing QTAIM calculations on actinide systems? A comparison of QTAIM metrics for $Cs_2UO_2Cl_4$, $U(Se_2PPh_2)_4$ and $Np(Se_2PPh_2)_4$ in gas phase, COSMO and PEECM

Joseph P. W. Wellington,[1] Andrew Kerridge[2] and Nikolas Kaltsoyannis*[3]


[1]Department of Chemistry, University College London,

20 Gordon Street, London, WC1H 0AJ, UK


[2]Department of Chemistry, Lancaster University, Bailrigg, Lancaster, LA1 4YP, UK


[3]School of Chemistry, The University of Manchester,

Oxford Road, Manchester, M13 9PL, UK


* nikolas.kaltsoyannis@manchester.ac.uk

Quantum Theory of Atoms-in-Molecules bond critical point and delocalisation index metrics are calculated for a range of actinide-element bonds in gas-phase, continuum solvent and *via* an electrostatic embedded cluster approach.

1
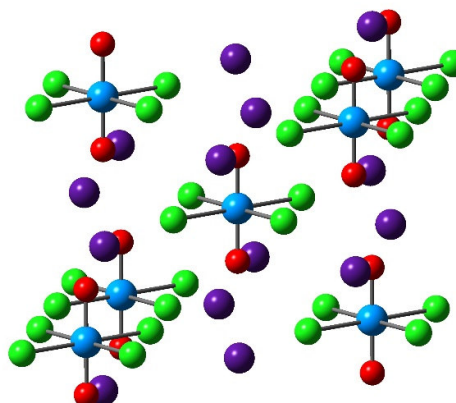
**Abstract**

Quantum Theory of Atoms-in-Molecules bond critical point and delocalisation index metrics are calculated for the actinide-element bonds in $Cs_2UO_2Cl_4$, $U(Se_2PPh_2)_4$ and $Np(Se_2PPh_2)_4$, in gas-phase, continuum solvent (COSMO) and *via* the periodic electrostatic embedded cluster method. The effects of the environment are seen to be very minor, suggesting that they do not account for the differences previously observed between the experimental and theoretical QTAIM $\rho_b$ and $\nabla^2\rho_b$ for the U-O bonds in $Cs_2UO_2Cl_4$. With the exception of the local density approximation, there is only a small dependence of the QTAIM metrics on the exchange-correlation functional employed.

**Introduction**

When probing chemical bonding, it can sometimes be difficult to make connections between the results from experiment and properties calculated from quantum chemistry. Standard quantum chemical properties such as partial atomic charges and bond orders are not directly observable experimentally and, while experimental techniques are available for determining atomic orbital mixing (*e.g.* ligand K-edge X-ray Absorption Spectroscopy[1,2] and Photoelectron Spectroscopy[3]) there is no unique computational way to express molecular orbital structure, with conclusions drawn from analysis of canonical orbitals often being rather different from those obtained from localised orbital descriptions. These difficulties make analysis of electron density an attractive alternative, as it is a physical observable which may be derived from experiment and calculated quantum chemically. The Quantum Theory of Atoms-in-Molecules (QTAIM)[4], which focuses on the topology of the electron density, provides a direct link between results from experiment and theory, and such comparisons are by now well established,[5] with many studies of organic and inorganic systems.

The 5f series, however, is an area of the periodic table for which QTAIM comparisons between theory and experiment are almost non-existent. This is due partly to the experimental difficulties associated with obtaining high quality experimental electron densities on radioactive systems featuring very heavy elements, and partly a function of the QTAIM only recently being extended to quantum chemical studies of the actinide elements. Indeed, we were the first group to extensively employ the QTAIM in this capacity, and have used it to study both covalency[6–18] and bond strength[19–21] in a range of molecular f element systems.

$Th(S_2PMe_2)_4$[22] and $Cs_2UO_2Cl_4$[23,24] are the only actinide systems to have been studied experimentally using the QTAIM. Zhurov *et al.* obtained the electron density of $Cs_2UO_2Cl_4$ from accurate X-ray diffraction experiments, and subsequently performed QTAIM analysis. Vallet *et al.* then carried out a quantum chemical study of $[UO_2Cl_4]^{2-}$ using density functional theory (DFT), and probed the electron density topology using the QTAIM.[25] The electron density $\rho$ and its Laplacian $\nabla^2\rho$ at the bond critical points of the U-Cl bonds were found to be in good agreement between theory and experiment. However, for the U-O bond they differ by 0.06 a.u. (24%) and

3

0.33 a.u. (51%) respectively. As the quantum chemical electron density was obtained from calculation of $[UO_2Cl_4]^{2-}$ in the gas phase, it was suggested that the differences could be related to the long-range influence of the crystal field.[25] Little is known about this; an earlier theoretical study of the effects of the crystal field on the topology of the electron density of methyl lithium[26] found it to be fairly modest. This study analysed calculations performed in the gas phase, with a polarizable continuum solvent model, with the Periodic Electrostatic Embedded Cluster Method (PEECM)[27] and with periodic boundary conditions; $\rho$ and $\nabla^2\rho$ did not vary significantly between the methods, though no comparison was made with experiment. Other studies on organic molecules also found only small differences between molecular and periodic boundary condition DFT calculations.[28,29]

Parenthetically, we note that Vallet *et al.* have previously studied the effect of environment on the electronic spectrum of the uranyl dication ($UO_2^{2+}$) in $Cs_2UO_2Cl_4$.[30] The most significant environmental effects were found to be due to the equatorial chloride ligands, with only small contributions from the crystal environment.

The aim of the present study is to investigate the effect of long range interactions on QTAIM parameters in 5f systems, and to establish if better representing these interactions leads to improved agreement between theory and experiment. We target $Cs_2UO_2Cl_4$, and $U(Se_2PPh_2)_4$ and $Np(Se_2PPh_2)_4$, which have also recently been studied by the QTAIM.[11] The electron densities are obtained from calculations in the gas-phase, in a polarizable continuum with the Conductor-Like Screening Model (COSMO)[31] and embedded in point charges with the PEECM. Should environmental effects reduce the differences between theory and experiment it is clear that including them will be important in future QTAIM studies. By contrast, if it is seen that the surrounding medium has little effect on the QTAIM data then we would be confident in recommending it sufficient to perform QTAIM analysis on electron densities from gas phase calculations.

4

**Computational Details and Methodology**

All quantum chemical calculations were performed using density functional theory (DFT) as implemented in the TURBOMOLE 6.5 program[32]. As the B3LYP exchange-correlation functional was used in the previous theoretical study of $[UO_2Cl_4]^{2-}$ [25] it has also been employed in the present calculations. The functional dependence of the QTAIM parameters was probed with a range of exchange-correlation functionals: B3LYP[33], LDA (VWN)[34], PBE[35], PBE0[36], TPSS[37] and TPSSH[38]. The self-consistent field convergence criterion was set to $1 \times 10^{-6}$.

The def-TZVPP basis sets contained in the TURBOMOLE library were used for all O, Se, P, C and H atoms[39], whilst the SARC-DKH basis sets were used for U[40], Np[40] and Cs (taken from the ORCA[41] basis set library).

Experimental crystal structures for $Cs_2UO_2Cl_4$[23], $U(Se_2PPh_2)_4$[11] and $Np(Se_2PPh_2)_4$[11] were used to provide the atomic positions, as well as the positions of the point charges in the embedding regions for the PEECM.

Wavefunction files were analysed with AIMAll version 14[42].

COSMO calculations were performed using the TURBOMOLE 6.5 default parameters, *i.e.* a relative permittivity of $\varepsilon_r = \infty$ and molecular cavities constructed of spheres of radius 2.223 Å for U, Np and Cs, 1.720 Å for O, 2.050 Å for Cl, 2.200 Å for Se, 2.106 Å for P, 2.000 Å for C and 1.300 Å for H.

*PEECM*

In order to incorporate long range crystal field effects, calculations were performed using the PEECM[27] as implemented in TURBOMOLE 6.5. The PEECM splits the system into two regions; an inner explicit cluster region treated quantum mechanically as described above and an infinite outer embedding region consisting of point charges, which recreates the Madelung potential of the bulk system. The latter region is itself often split to include an intermediate region immediately surrounding the QM cluster in which pseudopotentials (PPs) replace the positive point charges. These PPs are employed in order to avoid overpolarization of the electron density in the inner explicit cluster region. In the present study, however, we have not included an intermediate region as the wfn files required for QTAIM analysis must be generated using all-electron basis sets. Hence in order to probe, and if necessary mitigate, overpolarisation of the QM electron density, point charges

5

in the embedding region have been assigned either formal or natural charges. The formal charges for $Cs_2UO_2Cl_4$ are +1, +6, -2 and -1 for Cs, U, O and Cl respectively. The natural charges used for the $[UO_2Cl_4]^{2-}$, $Cs_2UO_2Cl_4$ and $(Cs_2UO_2Cl_4)_7$ calculations were obtained from the natural charges of the central $Cs_2UO_2Cl_4$ unit in a series of iterative $(Cs_2UO_2Cl_4)_7$ calculations. The iterative $(Cs_2UO_2Cl_4)_7$ calculations involved embedding the $(Cs_2UO_2Cl_4)_7$ system in an infinite array of formal charges within the PEECM framework, then taking the natural charges obtained on the central $Cs_2UO_2Cl_4$ unit to redefine the charges in the embedding region. The process was repeated until the natural charges were converged to 0.01 a.u. The natural charges for the central $Cs_2UO_2Cl_4$ unit and hence used for the embedding are +0.96, +1.20, -0.68 and -0.44 for Cs, U, O and Cl respectively. The formal charges for $U(Se_2PPh_2)_4$ and $Np(Se_2PPh_2)_4$ are +4, -1, +1, 0 and 0 on U, Se, P, C and H respectively. The natural charges used for the two systems were again obtained from an iterative process. Two sets of natural charges were obtained for the C atoms, one for those in the phenyl ring which are bonded to P atoms and another for all the other C atoms in the phenyl ring. The natural charges for $U(Se_2PPh_2)_4$ and so used for the embedding are -0.68, -0.23, 1.09, -0.16 and 0.19 on U, Se, P, C and H respectively, C atoms bonded to P have a natural charge of -0.38. The natural charges for $Np(Se_2PPh_2)_4$ and so used for the embedding are -0.60, -0.20, +1.07, -0.16 and 0.18 on Np, Se, P, C and H respectively, C atoms bonded to P have a natural charge of -0.36.

6

**Results and Discussion**

*Cs₂UO₂Cl₄*

As noted in the Introduction, Vallet *et al.* studied $[UO_2Cl_4]^{2-}$ quantum chemically;[25] here we calculate $[UO_2Cl_4]^{2-}$ as well as $Cs_2UO_2Cl_4$ and a cluster of seven formula units $(Cs_2UO_2Cl_4)_7$ in which the central $[UO_2Cl_4]^{2-}$ anion is surrounded by the next nearest six $[UO_2Cl_4]^{2-}$ units, along with the nearest 14 Cs atoms to make the cluster neutral (Figure 1). These three systems have been considered in the gas phase, in a polarizable continuum solvent model with COSMO and embedded in point charges with the PEECM. Both natural charges, obtained from an iterative natural population analysis, and formal charges have been used to define the values of the point charges in the PEECM. The electron densities obtained from these calculations have been analysed using the QTAIM, and the results are shown in Table 1 and 2.
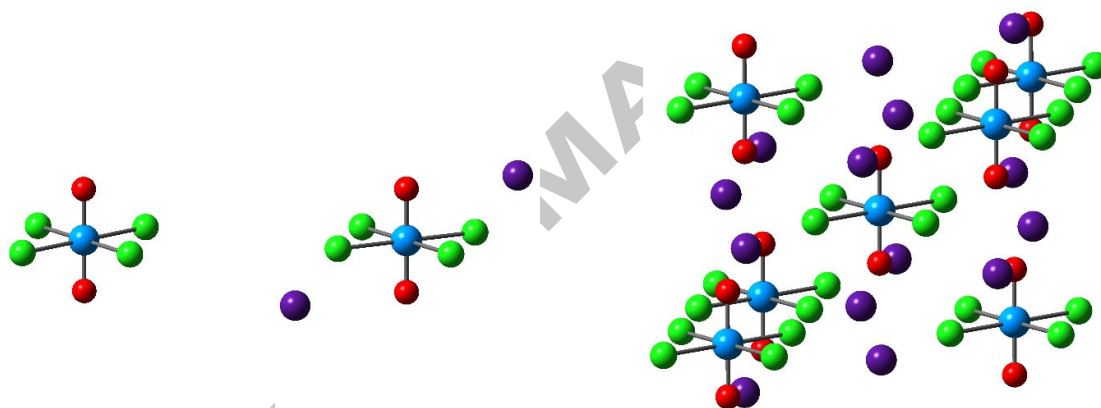


**Figure 1.** Ball and stick images of $[UO_2Cl_4]^{2-}$ (left), $Cs_2UO_2Cl_4$ (centre) and $(Cs_2UO_2Cl_4)_7$ (right). Chlorine atoms are shown in green, caesium atoms in purple, oxygen atoms in red and uranium atoms in blue. Atomic positions are taken from experiment[23].

The QTAIM states that there is a bond critical point (BCP) between every two atoms bonded to each other, with the BCP located at the minimum in the electron density along the bond path, the line of maximum electron density between the two atoms.[4] The values of $\rho$, $\nabla^2\rho$, and the energy density, $H$, at the BCP can be used in analysing the nature of the bond. A value of $\rho$ at the BCP ($\rho_b$) greater than 0.2 a.u. is a sign of a covalent interaction, whereas values less than 0.1 a.u. indicate a closed shell interaction such as ionic, hydrogen or Van der Waals bonding. A positive $\nabla^2\rho_b$ value means there is a depletion of charge at the BCP whilst a negative value means there is a local charge concentration and indicates a covalent interaction. $H_b$ is negative for interactions with sharing of electrons, with its magnitude indicating the covalency of

7

the interaction.[43] A bond is cylindrically symmetric when the bond ellipticity $\varepsilon$ is 0, such as in single and triple bonds, with higher values otherwise. The delocalisation index *DI* between two bonded atoms gives an indication of the bond order between them.

In both this and previous studies the values of $\rho_b$ for the U-O bonds are all greater than 0.2 a.u. and the relatively large, negative $H_b$ support a strongly covalent description (Table 1). The values of $\rho_b$ are similar to those found for M≡O (M = Cr, Mo and W) triple bonds.[44] The values of $\varepsilon$ so close to zero suggest a triple bond for U-O, in keeping with a $\sigma + 2\pi$ description. The strongly polar nature of the U–O bond accounts for the *DI* values (c. 1.9) being significantly lower than the formal value of 3 expected for a triple bond. The experimental papers suggest that the U-Cl bond can be described as partially covalent[23,24]; however, as also noted by Vallet *et al.*[25], the small absolute values of $H_b$ and $\rho_b$ indicate a largely ionic interaction (Table 2).

There are small differences of approximately 0.01 and 0.03 a.u in $\rho_b$ and $\nabla^2\rho_b$ for both bonds between our results and those of Vallet *et al.* These are likely to arise from the difference in geometry; whereas in the previous study the $[UO_2Cl_4]^{2-}$ unit was optimized, we have kept the geometry fixed at the experimentally-determined structure.

The results in Table 1 and 2 show that whether the clusters are in the gas-phase, a polarizable continuum solvent model or embedded in point charges has little effect on the topology of the electron density. For both the U-O and the U-Cl bonds in $[UO_2Cl_4]^{2-}$ the values of $\rho_b$, $\nabla^2\rho_b$ and $H_b$ differ by less than 0.01 a.u. in the different environments. Nor do the QTAIM data change greatly between the different systems; for the gas phase calculation the values of $\rho_b$, $\nabla^2\rho_b$ and $H_b$ differ by less than 0.01 a.u. between $[UO_2Cl_4]^{2-}$, $Cs_2UO_2Cl_4$ and $(Cs_2UO_2Cl_4)_7$.

8

| | $\rho_b$ (a.u.) | % | $\nabla^2\rho_b$ (a.u.) | % | $H_b$ (a.u.) | % | $\varepsilon$ | % | DI | % |
|---|---|---|---|---|---|---|---|---|---|---|
| **[UO$_2$Cl$_4$]$^{2-}$** | | | | | | | | | | |
| Gas phase | 0.303 | | 0.345 | | -0.272 | | 0.002 | | 1.881 | |
| COSMO | 0.303 | 0.0 | 0.344 | -0.5 | -0.272 | 0.0 | 0.002 | 31.6 | 1.871 | -0.5 |
| PEECM Natural | 0.302 | -0.2 | 0.350 | 1.2 | -0.272 | -0.3 | 0.005 | 189.2 | 1.882 | 0.0 |
| PEECM Formal | 0.302 | -0.2 | 0.350 | 1.3 | -0.271 | -0.3 | 0.003 | 39.4 | 1.879 | -0.1 |
| **Cs$_2$UO$_2$Cl$_4$** | | | | | | | | | | |
| Gas phase | 0.303 | | 0.343 | | -0.273 | | 0.004 | | 1.882 | |
| COSMO | 0.303 | -0.1 | 0.343 | 0.0 | -0.273 | -0.2 | 0.000 | -92.1 | 1.874 | -0.4 |
| PEECM Natural | 0.302 | -0.3 | 0.349 | 1.9 | -0.272 | -0.5 | 0.006 | 47.3 | 1.880 | -0.1 |
| PEECM Formal | 0.302 | -0.4 | 0.350 | 2.0 | -0.271 | -0.6 | 0.003 | -30.6 | 1.875 | -0.4 |
| **(Cs$_2$UO$_2$Cl$_4$)$_7$** | | | | | | | | | | |
| Gas phase | 0.303 | | 0.347 | | -0.273 | | 0.008 | | 1.877 | |
| COSMO | 0.303 | 0.1 | 0.345 | -0.5 | -0.273 | 0.1 | 0.006 | -22.3 | 1.877 | 0.0 |
| PEECM Natural | 0.303 | 0.0 | 0.346 | -0.3 | -0.273 | 0.0 | 0.006 | -28.2 | 1.870 | -0.4 |
| Experiment[24] | 0.25 | | 0.65 | - | -0.23 | | - | | - | |
| Previous DFT[25] | 0.31 | | 0.32 | - | -0.27 | | - | | 1.92 | |

**Table 1**. QTAIM BCP and *DI* data for the U-O bonds in [UO$_2$Cl$_4$]$^{2-}$, Cs$_2$UO$_2$Cl$_4$ and the central [UO$_2$Cl$_4$]$^{2-}$ unit in (Cs$_2$UO$_2$Cl$_4$)$_7$. Each system is calculated in the gas phase, with a polarizable continuum solvent model *via* the COSMO and with the PEECM with natural and formal charges in the embedding region. $\rho_b$, $\nabla^2\rho_b$ and $H_b$ in atomic units. Percentage differences from the gas phase data are given in the columns to the right of each metric. No values are available for (Cs$_2$UO$_2$Cl$_4$)$_7$ with PEECM in formal charges due to SCF convergence difficulties.

| | $\rho_b$ (a.u.) | % | $\nabla^2\rho_b$ (a.u.) | % | $H_b$ (a.u.) | % | $\varepsilon$ | % | DI | % |
|---|---|---|---|---|---|---|---|---|---|---|
| **[UO$_2$Cl$_4$]$^{2-}$** | | | | | | | | | | |
| Gas phase | 0.061 | | 0.146 | | -0.011 | | 0.054 | | 0.571 | |
| COSMO | 0.062 | 0.6 | 0.145 | -0.6 | -0.011 | 1.7 | 0.055 | 2.5 | 0.580 | 1.6 |
| PEECM Natural | 0.062 | 0.5 | 0.145 | -0.3 | -0.011 | 1.4 | 0.058 | 7.7 | 0.574 | 0.5 |
| PEECM Formal | 0.062 | 0.7 | 0.145 | -0.5 | -0.011 | 2.2 | 0.057 | 5.5 | 0.577 | 1.0 |
| **Cs$_2$UO$_2$Cl$_4$** | | | | | | | | | | |
| Gas phase | 0.062 | | 0.146 | | -0.011 | | 0.055 | | 0.574 | |
| COSMO | 0.062 | 0.3 | 0.145 | -0.3 | -0.011 | 0.9 | 0.055 | -1.0 | 0.578 | 0.8 |
| PEECM Natural | 0.062 | 0.1 | 0.145 | -0.3 | -0.011 | 0.6 | 0.056 | 1.4 | 0.573 | -0.1 |
| PEECM Formal | 0.062 | 0.5 | 0.145 | -0.7 | -0.011 | 1.7 | 0.053 | -3.3 | 0.575 | 0.3 |
| **(Cs$_2$UO$_2$Cl$_4$)$_7$** | | | | | | | | | | |
| Gas phase | 0.061 | | 0.147 | | -0.011 | | 0.058 | | 0.556 | |
| COSMO | 0.062 | 0.1 | 0.146 | -0.1 | -0.011 | 0.4 | 0.056 | -2.7 | 0.558 | 0.4 |
| PEECM Natural | 0.062 | 0.3 | 0.146 | -0.3 | -0.011 | 1.0 | 0.055 | -5.4 | 0.562 | 1.1 |
| Expt[24] | 0.07 | | 0.14 | | -0.03 | | - | | - | |
| Prev DFT[25] | 0.05 | | 0.12 | | -0.01 | | - | | 0.53 | |

**Table 2**. QTAIM BCP and *DI* data for the U-Cl bonds in [UO$_2$Cl$_4$]$^{2-}$, Cs$_2$UO$_2$Cl$_4$ and the central [UO$_2$Cl$_4$]$^{2-}$ unit in (Cs$_2$UO$_2$Cl$_4$)$_7$. Each system is calculated in the gas phase, with a polarizable continuum solvent model *via* the COSMO and with the PEECM with natural and formal charges in the embedding region. $\rho_b$, $\nabla^2\rho_b$ and $H_b$ in atomic units. Percentage differences from the gas phase data are given in the columns to the right of each metric. No values are available for (Cs$_2$UO$_2$Cl$_4$)$_7$ with PEECM in formal charges due to SCF convergence difficulties.

9

Götz *et al.* who, as noted in the Introduction, performed a similar theoretical study comparing QTAIM values for methyl lithium in different environments but with the same experimental geometry, saw changes of up to 10.8% and 3.3% in the $\rho_b$ of Li-C and C-H bonds respectively[26] between the gas phase and embedding in point charges *via* the PEECM. These changes are larger than those found here for the U-O and U-Cl bonds which change by less than 1% between the polarizable continuum solvent model and the PEECM. The differences found in $\nabla^2\rho_b$ for methyl lithium were up to 1.2% and 6.7% for the Li-C and C-H bonds respectively, slightly larger than our differences (up to 2.0% for the U-O bonds). The percentage changes in $\varepsilon$ for U-O bond are very large, but as the absolute data are so small these percentage changes are arguably not meaningful.

The differences in the QTAIM data for the U-O bonds between gas phase, COSMO and PEECM calculations are very small and much less than those between the theoretical and experimental data, indicating that the latter differences are unlikely to be due to long range electrostatic effects within the crystal. Experimental charge density distributions are generally refined with the Hansen-Coppens multipole model,[45] as was the case for $Cs_2UO_2Cl_4$[23,24]. In this model the experimental density is described by a superposition of atom-centred aspherical electron densities. However, several limitations in describing the electron density *via* the multipole model have been noted previously.[46] Furthermore, the multipole model requires multipole expansions to be selected for each atom, and it has been suggested that hexadecapolar expansions are required for d-elements, with hexacontatetrapole expansions being necessary for f-elements[46]. However, in the $Cs_2UO_2Cl_4$ experimental studies only hexadecapolar expansions were used for uranium[23,24].

Differences between QTAIM values obtained from theory and experiment using multipole models have also been reported in previous studies on organic molecules.[28,29,47] In these studies experimental values of the Laplacian were up to 1.3 a.u. higher than theory for C=O bonds and 0.5 a.u. lower for N-H bonds, and hence the present difference between experiment and theory of approximately 0.3 a.u. for $\nabla^2\rho_b$ in the U-O bonds is typical of the differences found in other bonds. Although differences between the experimental and theoretical values of $\rho_b$ were also noted in these studies, these were significantly smaller than for $\nabla^2\rho_b$. For

10

example, in the study by Rykounov *et al.*, the maximum difference in $\rho_b$ between theory and experiment was 0.04 a.u., with the largest differences seen for bonds involving N or O atoms[29].

We were interested to establish if there is a functional dependence of the QTAIM values and so re-calculated $[UO_2Cl_4]^{2-}$ in the gas phase with five other exchange-correlation functionals; the results are shown in Table 3 and 4. Leaving the LDA data aside, the variation in the QTAIM metrics is very small for the U-Cl bonds, with differences in $\rho_b$, $\nabla^2\rho_b$ and $H_b$ of less than 0.01 a.u. (< 1% for $\rho_b$, 2% for $\nabla^2\rho_b$ and 6% for $H_b$) between the different functionals. The functional dependence is slightly larger for $\nabla^2\rho_b$ and $H_b$ for the U-O bonds; < 0.08 a.u. and 0.02 a.u. respectively, the former corresponding to a change of 14% between the B3LYP and TPSS functionals. None of these differences between functionals is as large as the difference between the theoretical and experimental $\rho_b$ and $\nabla^2\rho_b$ data for the U-O bonds.

The differences between the LDA QTAIM data and those from the GGA and post-GGA functionals are much larger than between the latter, particularly for $\nabla^2\rho_b$ for U-O, and $H_b$ and *DI* for U-Cl, which have differences of 26.7%, 90.7% and 57.0% respectively compared with B3LYP. Clearly the electron density in these systems is described significantly differently at the LDA level when compared with GGA and beyond. Although the LDA functional gives better agreement with experiment for $\rho_b$ and $\nabla^2\rho_b$ of the U-O bonds, we suggest this is most likely coincidental.

11

| | $\rho_b$ (a.u.) | % | $\nabla^2\rho_b$ (a.u.) | % | $H_b$ (a.u.) | % | $\varepsilon$ | % | $DI$ | % |
|---|---|---|---|---|---|---|---|---|---|---|
| B3LYP | 0.303 | | 0.345 | | -0.272 | | 0.002 | | 1.881 | |
| LDA | 0.287 | -5.3 | 0.438 | 26.7 | -0.261 | -4.2 | 0.001 | -54.1 | 1.877 | -0.2 |
| PBE | 0.301 | -0.7 | 0.380 | 10.0 | -0.267 | -1.9 | 0.002 | 25.1 | 1.930 | 2.6 |
| PBE0 | 0.306 | 0.9 | 0.316 | -8.4 | -0.280 | 2.8 | 0.002 | 15.8 | 1.887 | 0.3 |
| TPSS | 0.299 | -1.2 | 0.392 | 13.5 | -0.264 | -3.0 | 0.002 | 19.0 | 1.920 | 2.1 |
| TPSSH | 0.301 | -0.5 | 0.365 | 5.7 | -0.270 | -0.9 | 0.002 | 16.4 | 1.905 | 1.2 |

**Table 3**. QTAIM BCP and *DI* data for the U-O bonds in $[UO_2Cl_4]^{2-}$, calculated in gas phase with different exchange-correlation functionals. Percentage differences from the B3LYP data are given in the columns to the right of each metric.

| | $\rho_b$ (a.u.) | % | $\nabla^2\rho_b$ (a.u.) | % | $H_b$ (a.u.) | % | $\varepsilon$ | % | $DI$ | % |
|---|---|---|---|---|---|---|---|---|---|---|
| B3LYP | 0.061 | | 0.146 | | -0.011 | | 0.054 | | 0.571 | |
| LDA | 0.072 | 17.4 | 0.118 | -18.8 | -0.021 | 90.7 | 0.018 | -66.7 | 0.896 | 57.0 |
| PBE | 0.062 | 0.7 | 0.143 | -1.9 | -0.011 | 2.1 | 0.061 | 14.6 | 0.626 | 9.7 |
| PBE0 | 0.062 | 1.0 | 0.145 | -0.6 | -0.011 | 5.6 | 0.058 | 8.1 | 0.563 | -1.4 |
| TPSS | 0.061 | -0.7 | 0.149 | 1.9 | -0.010 | -6.0 | 0.066 | 22.4 | 0.613 | 7.4 |
| TPSSH | 0.061 | -0.4 | 0.149 | 1.9 | -0.010 | -3.6 | 0.063 | 17.9 | 0.588 | 3.0 |

**Table 4.** QTAIM BCP and *DI* data for the U-Cl bonds in $[UO_2Cl_4]^{2-}$, calculated in gas phase with different exchange-correlation functionals. Percentage differences from the B3LYP data are given in the columns to the right of each metric.

12

*U(Se$_2$PPh$_2$)$_4$ and Np(Se$_2$PPh$_2$)$_4$*

In order to see if the similarities in the QTAIM data between gas phase and embedded calculations is true beyond [UO$_2$Cl$_4$]$^{2-}$, we have calculated analogous QTAIM metrics for U(Se$_2$PPh$_2$)$_4$ (Figure 2) and Np(Se$_2$PPh$_2$)$_4$, both of which we have previously studied with the QTAIM.[11] As for [UO$_2$Cl$_4$]$^{2-}$, Cs$_2$UO$_2$Cl$_4$ and (Cs$_2$UO$_2$Cl$_4$)$_7$, the QTAIM data have been calculated for An(Se$_2$PPh$_2$)$_4$ in the gas phase, in a polarizable continuum with COSMO and embedded in point charges (both natural and formal) with the PEECM. The average values for the An-Se, Se-P and P-C bonds, as well as the C-H bonds of the carbons in the para position of the phenyl ring (chosen as these bonds are closest to the edge of the QM region), are collected in Tables 5-8 respectively.
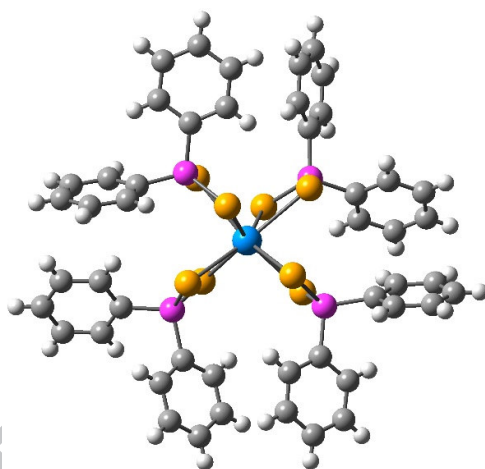


**Figure 2.** Ball and stick representation of U(Se$_2$PPh$_2$)$_4$, Carbon atoms are shown in grey, hydrogen atoms in white, phosphorus atoms in pink, sulfur atoms in yellow and the uranium atom in blue. Atomic positions taken from reference[11].

As noted previously[11], the small values of $\rho_b$ and $H_b$ for the actinide-selenium bonds calculated in gas phase indicate that these are mostly ionic. These conclusions are unaltered by the effects of COSMO solvation or embedding *via* the PEECM, especially so for the An-Se and para C-H bonds which have less than a 1% change in their $\rho_b$, $\nabla^2\rho_b$ and $H_b$ values, corresponding to differences of less than 0.01 a.u. in $\rho_b$ and $H_b$ and less than 0.02 a.u. in $\nabla^2\rho_b$. The Se-P and P-C bonds show larger changes in $\nabla^2\rho_b$, with up to 5% difference for the Se-P bond and 9% difference for the P-C bond, most notably for the COSMO calculations. However, even these changes are still rather modest, and it is worth noting that the changes are similar

between the uranium and neptunium systems; hence a comparative trend in QTAIM data between actinides is largely unaffected by the environment.

|  |  | $\rho_b$ (a.u.) | % | $\nabla^2\rho_b$ (a.u.) | % | $H_b$ (a.u.) | % | $\varepsilon$ | % | DI | % |
|---|---|---|---|---|---|---|---|---|---|---|---|
| U(Se$_2$PPh$_2$)$_4$ | Gas phase | 0.045 |  | 0.063 |  | -0.008 |  | 0.174 |  | 0.495 |  |
|  | COSMO | 0.045 | -0.1 | 0.063 | 0.1 | -0.008 | -0.5 | 0.167 | -4.3 | 0.499 | 0.8 |
|  | PEECM Natural | 0.045 | -0.1 | 0.063 | -0.1 | -0.008 | -0.1 | 0.162 | -6.9 | 0.495 | 0.0 |
|  | PEECM Formal | 0.045 | -0.1 | 0.063 | -0.1 | -0.008 | -0.1 | 0.160 | -8.2 | 0.495 | 0.0 |
| Np(Se$_2$PPh$_2$)$_4$ | Gas phase | 0.045 |  | 0.065 |  | -0.008 |  | 0.159 |  | 0.505 |  |
|  | COSMO | 0.045 | -0.1 | 0.065 | 0.2 | -0.008 | -0.5 | 0.155 | -2.5 | 0.505 | 0.0 |
|  | PEECM Natural | 0.045 | 0.0 | 0.065 | 0.1 | -0.008 | -0.1 | 0.154 | -2.9 | 0.505 | 0.1 |
|  | PEECM Formal | 0.045 | 0.0 | 0.065 | 0.1 | -0.008 | -0.1 | 0.157 | -1.4 | 0.505 | 0.0 |

**Table 5**. QTAIM BCP and *DI* data for the An-Se bond in U(Se$_2$PPh$_2$)$_4$ and Np(Se$_2$PPh$_2$)$_4$. Both systems are calculated in the gas phase, with a polarizable continuum solvent model *via* the COSMO and with the PEECM with natural and formal charges in the embedding region. $\rho_b$, $\nabla^2\rho_b$ and $H_b$ in atomic units. Percentage differences from the gas phase data are given in the columns to the right of each metric.

|  |  | $\rho_b$ (a.u.) | % | $\nabla^2\rho_b$ (a.u.) | % | $H_b$ (a.u.) | % | $\varepsilon$ | % | DI | % |
|---|---|---|---|---|---|---|---|---|---|---|---|
| U(Se$_2$PPh$_2$)$_4$ | Gas phase | 0.131 |  | -0.123 |  | -0.075 |  | 0.026 |  | 1.170 |  |
|  | COSMO | 0.131 | 0.2 | -0.128 | 4.2 | -0.075 | 0.5 | 0.023 | -12.3 | 1.158 | -1.0 |
|  | PEECM Natural | 0.131 | 0.1 | -0.125 | 1.7 | -0.075 | 0.2 | 0.024 | -6.5 | 1.165 | -0.4 |
|  | PEECM Formal | 0.131 | 0.0 | -0.124 | 0.7 | -0.075 | 0.1 | 0.026 | -1.7 | 1.168 | -0.2 |
| Np(Se$_2$PPh$_2$)$_4$ | Gas phase | 0.131 |  | -0.125 |  | -0.076 |  | 0.031 |  | 1.170 |  |
|  | COSMO | 0.132 | 0.2 | -0.131 | 4.2 | -0.076 | 0.5 | 0.027 | -11.5 | 1.158 | -1.0 |
|  | PEECM Natural | 0.132 | 0.1 | -0.128 | 1.7 | -0.076 | 0.2 | 0.029 | -5.0 | 1.165 | -0.4 |
|  | PEECM Formal | 0.132 | 0.0 | -0.127 | 0.8 | -0.076 | 0.1 | 0.030 | -2.0 | 1.168 | -0.2 |

**Table 6**. QTAIM BCP and *DI* data for the Se-P bond in U(Se$_2$PPh$_2$)$_4$ and Np(Se$_2$PPh$_2$)$_4$. Both systems are calculated in the gas phase, with a polarizable continuum solvent model *via* the COSMO and with the PEECM with natural and formal charges in the embedding region. $\rho_b$, $\nabla^2\rho_b$ and $H_b$ in atomic units. Percentage differences from the gas phase data are given in the columns to the right of each metric.

15

| | | $\rho_b$ (a.u.) | % | $\nabla^2\rho_b$ (a.u.) | % | $H_b$ (a.u.) | % | $\varepsilon$ | % | $DI$ | % |
|---|---|---|---|---|---|---|---|---|---|---|---|
| U(Se₂PPh₂)₄ | Gas phase | 0.172 | | -0.215 | | -0.175 | | 0.067 | | 0.777 | |
| | COSMO | 0.173 | 0.4 | -0.234 | 8.5 | -0.176 | 0.8 | 0.069 | 3.7 | 0.786 | 1.2 |
| | PEECM Natural | 0.172 | 0.2 | -0.223 | 3.6 | -0.175 | 0.3 | 0.068 | 1.4 | 0.781 | 0.5 |
| | PEECM Formal | 0.172 | 0.1 | -0.218 | 1.3 | -0.175 | 0.1 | 0.067 | 0.6 | 0.778 | 0.2 |
| Np(Se₂PPh₂)₄ | Gas phase | 0.173 | | -0.208 | | -0.178 | | 0.066 | | 0.773 | |
| | COSMO | 0.173 | 0.5 | -0.226 | 8.8 | -0.177 | -0.2 | 0.069 | 3.5 | 0.783 | 1.2 |
| | PEECM Natural | 0.173 | 0.2 | -0.216 | 3.7 | -0.176 | -0.7 | 0.067 | 1.4 | 0.777 | 0.5 |
| | PEECM Formal | 0.173 | 0.1 | -0.211 | 1.6 | -0.176 | -0.9 | 0.067 | 0.7 | 0.775 | 0.2 |

**Table 7**. QTAIM BCP and DI data for the P-C bond in U(Se₂PPh₂)₄ and Np(Se₂PPh₂)₄. Both systems are calculated in the gas phase, with a polarizable continuum solvent model *via* the COSMO and with the PEECM with natural and formal charges in the embedding region. $\rho_b$, $\nabla^2\rho_b$ and $H_b$ in atomic units. Percentage differences from the gas phase data are given in the columns to the right of each metric.

| | | $\rho_b$ (a.u.) | % | $\nabla^2\rho_b$ (a.u.) | % | $H_b$ (a.u.) | % | $\varepsilon$ | % | $DI$ | % |
|---|---|---|---|---|---|---|---|---|---|---|---|
| U(Se₂PPh₂)₄ | Gas phase | 0.406 | | -2.016 | | -0.617 | | 0.001 | | 1.001 | |
| | COSMO | 0.408 | 0.6 | -2.037 | 1.1 | -0.615 | -0.3 | 0.001 | -45.7 | 0.998 | -0.3 |
| | PEECM Natural | 0.407 | 0.3 | -2.029 | 0.6 | -0.616 | -0.2 | 0.001 | 25.1 | 1.000 | -0.2 |
| | PEECM Formal | 0.407 | 0.2 | -2.025 | 0.5 | -0.616 | -0.1 | 0.001 | 12.6 | 0.999 | -0.2 |
| Np(Se₂PPh₂)₄ | Gas phase | 0.405 | | -2.008 | | -0.616 | | 0.002 | | 0.999 | |
| | COSMO | 0.407 | 0.6 | -2.029 | 1.0 | -0.614 | -0.3 | 0.003 | 19.8 | 0.995 | -0.3 |
| | PEECM Natural | 0.406 | 0.3 | -2.020 | 0.6 | -0.615 | -0.2 | 0.003 | 16.6 | 0.997 | -0.1 |
| | PEECM Formal | 0.406 | 0.2 | -2.016 | 0.4 | -0.616 | -0.1 | 0.003 | 18.1 | 0.997 | -0.2 |

**Table 8**. QTAIM BCP and DI data for the para C-H bond in U(Se₂PPh₂)₄ and Np(Se₂PPh₂)₄. Both systems are calculated in the gas phase, with a polarizable continuum solvent model *via* the COSMO and with the PEECM with natural and formal charges in the embedding region. $\rho_b$, $\nabla^2\rho_b$ and $H_b$ in atomic units. Percentage differences from the gas phase data are given in the columns to the right of each metric.

16

## Conclusions

Intrigued by the suggestion that environmental effects account for the differences observed in the experimental and theoretical QTAIM $\rho_b$ and $\nabla^2\rho_b$ for the U-O bonds in $Cs_2UO_2Cl_4$, we have investigated the effects of environment on the QTAIM metrics of bonds in uranium and neptunium containing systems. These effects have been incorporated using the COSMO and PEECM approaches; both have very modest effects on the QTAIM data, and we conclude that they cannot account for the differences seen in $Cs_2UO_2Cl_4$. Rather, we suggest that these differences may be due to deficiencies in the refinement of experimental electron density data *via* the multipole model, as has been previously seen in organic systems. Our data strongly suggest that QTAIM studies of molecular electron densities calculated in gas phase are adequate for the study of actinide systems, and also that, once beyond the local density approximation, there is only a small dependence of the QTAIM metrics on the exchange-correlation functional employed.

## Acknowledgements

## References

[1] E.I. Solomon, B. Hedman, K.O. Hodgson, A. Dey, R.K. Szilagyi, Coord. Chem. Rev. 249 (2005) 97–129. doi:10.1016/j.ccr.2004.03.020.

[2] M.L. Neidig, D.L. Clark, R.L. Martin, Coord. Chem. Rev. 257 (2013) 394–406. doi:10.1016/j.ccr.2012.04.029.

[3] J.C. Green, P. Decleva, Coord. Chem. Rev. 249 (2005) 209–228. doi:10.1016/j.ccr.2004.02.012.

[4] R.F.W. Bader, Atoms in Molecules: A Quantum Theory, Clarendon Press, Oxford, 1990.

[5] D. Chopra, J. Phys. Chem. A 116 (2012) 9791–9801. doi:10.1021/jp306169f.

[6] M.J. Tassell, N. Kaltsoyannis, Dalton Trans. 39 (2010) 6719–6725. doi:10.1039/c000704h.

[7] I. Kirker, N. Kaltsoyannis, Dalton Trans. 40 (2011) 124–131. doi:10.1039/C0DT01018A.

[8] M.P. Blake, N. Kaltsoyannis, P. Mountford, J. Am. Chem. Soc. 133 (2011) 15358–15361. doi:10.1021/ja207487j.

[9] N. Kaltsoyannis, Inorg. Chem. 52 (2013) 3407–3413. doi:10.1021/ic3006025.

[10] D.D. Schnaars, A.J. Gaunt, T.W. Hayton, M.B. Jones, I. Kirker, N. Kaltsoyannis, et al., Inorg. Chem. 51 (2012) 8557–8566. doi:10.1021/ic301109f.

[11] M.B. Jones, A.J. Gaunt, J.C. Gordon, N. Kaltsoyannis, M.P. Neu, B.L. Scott, Chem. Sci. 4 (2013) 1189–1203. doi:10.1039/c2sc21806b.

[12] D.E. Smiles, G. Wu, N. Kaltsoyannis, T.W. Hayton, Chem. Sci. 6 (2015) 3891–3899. doi:10.1039/C5SC01248A.

[13] P.L. Arnold, A. Prescimone, J.H. Farnaby, S.M. Mansell, S. Parsons, N. Kaltsoyannis, Angew. Chemie Int. Ed. 54 (2015) 6735–6739. doi:10.1002/anie.201411250.

[14] R. Beekmeyer, A. Kerridge, Inorganics 3 (2015) 482–499. doi:10.3390/inorganics3040482.

[15] A. Kerridge, Dalton Trans. 42 (2013) 16428–16436. doi:10.1039/c3dt52279b.

[16] A. Kerridge, RSC Adv. 4 (2014) 12078–12086. doi:10.1039/C3RA47088A.

[17] A.C. Behrle, C.L. Barnes, N. Kaltsoyannis, J.R. Walensky, Inorg. Chem. 52 (2013) 10623–10631. doi:10.1021/ic401642a.

[18] A.C. Behrle, A. Kerridge, J.R. Walensky, Inorg. Chem. 54 (2015) 11625–11636. doi:10.1021/acs.inorgchem.5b01342.

[19] A.R.E. Mountain, N. Kaltsoyannis, Dalton Trans. 42 (2013) 13477–13486. doi:10.1039/c3dt51337h.

[20] Q.-R. Huang, J.R. Kingham, N. Kaltsoyannis, Dalton Trans. 44 (2015) 2554–2566. doi:10.1039/C4DT02323D.

[21] P. Di Pietro, A. Kerridge, Inorg. Chem. 55 (2016) 573–583. doi:10.1021/acs.inorgchem.5b01219.

[22] B.B. Iversen, F.K. Larsen, A.A. Pinkerton, A. Martin, A. Darovsky, P.A. Reynolds, Acta Crystallogr. Sect. B Struct. Sci. 55 (1999) 363–374. doi:10.1107/S0108768198010398.

[23] V. V. Zhurov, E.A. Zhurova, A.I. Stash, A.A. Pinkerton, J. Phys. Chem. A 115 (2011) 13016–13023. doi:10.1021/jp204965b.

[24] V. V. Zhurov, E.A. Zhurova, A.A. Pinkerton, Inorg. Chem. 50 (2011) 6330–6333. doi:10.1021/ic200759u.

[25] V. Vallet, U. Wahlgren, I. Grenthe, J. Phys. Chem. A 116 (2012) 12373–12380. doi:10.1021/jp3091123.

[26] K. Götz, F. Meier, C. Gatti, A.M. Burow, M. Sierka, J. Sauer, et al., J. Comput. Chem. 31 (2010) 2568–2576. doi:10.1002/jcc.21548.

[27] A.M. Burow, M. Sierka, J. Döbler, J. Sauer, J. Chem. Phys. 130 (2009) 174710. doi:10.1063/1.3123527.

[28] A. Volkov, Y. Abramov, P. Coppens, C. Gatti, Acta Crystallogr. Sect. A Found. Crystallogr. 56 (2000) 332–339. doi:10.1107/S0108767300003202.

[29] A.A. Rykounov, A.I. Stash, V. V. Zhurov, E.A. Zhurova, A.A. Pinkerton, V.G. Tsirelson, Acta Crystallogr. Sect. B Struct. Sci. 67 (2011) 425–436. doi:10.1107/S0108768111033015.

[30] A.S.P. Gomes, C.R. Jacob, F. Réal, L. Visscher, V. Vallet, Phys. Chem. Chem. Phys. 15 (2013) 15153–62. doi:10.1039/c3cp52090k.

[31] A. Klamt, G. Schüürmann, J. Chem. Soc. Perkin Trans. 2 (1993) 799–805. doi:10.1039/p29930000799.

[32] R. Ahlrichs, M. Bär, M. Häser, H. Horn, C. Kölmel, Chem. Phys. Lett. 162 (1989) 165–169. doi:10.1016/0009-2614(89)85118-8.

[33] A.D. Becke, J. Chem. Phys. 98 (1993) 5648–5652. doi:10.1063/1.464913.

[34] S.H. Vosko, L. Wilk, M. Nusair, Can. J. Phys. 58 (1980) 1200 –1211.

[35] J.P. Perdew, K. Burke, M. Ernzerhof, Phys. Rev. Lett. 78 (1997) 1396–1396. doi:10.1103/PhysRevLett.78.1396.

[36] J.P. Perdew, M. Ernzerhof, K. Burke, J. Chem. Phys. 105 (1996) 9982–9985. doi:10.1063/1.472933.

[37] J. Tao, J.P. Perdew, V.N. Staroverov, G.E. Scuseria, Phys. Rev. Lett. 91 (2003) 146401–146404. doi:10.1103/PhysRevLett.91.146401.

[38] V.N. Staroverov, G.E. Scuseria, J. Tao, J.P. Perdew, J. Chem. Phys. 119 (2003) 12129–12137. doi:10.1063/1.1626543.

[39] F. Weigend, M. Häser, H. Patzelt, R. Ahlrichs, Chem. Phys. Lett. 294 (1998) 143–152. doi:10.1016/S0009-2614(98)00862-8.

[40] D.A. Pantazis, F. Neese, J. Chem. Theory Comput. 7 (2011) 677–684. doi:10.1021/ct100736b.

[41]  F. Neese, Wiley Interdiscip. Rev. Comput. Mol. Sci. 2 (2012) 73–78. doi:10.1002/wcms.81.

[42]  T.A. Keith, TK Gristmill Softw. 14.11.23 (2014) .

[43]  D. Cremer, E. Kraka, Angew. Chemie Int. Ed. English 23 (1984) 627–628. doi:10.1002/anie.198406271.

[44]  C.-C. Wang, T. Tang, Y. Wang, J. Phys. Chem. A 104 (2000) 9566–9572. doi:10.1021/jp001130x.

[45]  N.K. Hansen, P. Coppens, Acta Crystallogr. Sect. A Cryst. Physics, Diffraction, Theor. Gen. Crystallogr. 34 (1978) 909–921. doi:10.1107/S0567739478001886.

[46]  P. Macchi, J.-M. Gillet, F. Taulelle, J. Campo, N. Claiser, C. Lecomte, IUCrJ 2 (2015) 441–451. doi:10.1107/S2052252515007538.

[47]  B. Dittrich, S. Scheins, C. Paulmann, P. Luger, J. Phys. Chem. A 107 (2003) 7471–7474. doi:10.1021/jp022584s.